

Research Article

Silicon Carbide-Derived Carbon Prepared by Fused Salt Electrolysis and Electrochemical Performance

Shuyuan Wang¹ and Guangjie Shao²

¹School of Chemical Engineering, Hebei Normal University of Science and Technology, Qinhuangdao 066004, China

²State key Laboratory of Metastable Materials Science and Technology, Yanshan University, Qinhuangdao 066004, China

Correspondence should be addressed to Guangjie Shao; shaogj@ysu.edu.cn

Received 30 March 2016; Revised 18 May 2016; Accepted 1 June 2016

Academic Editor: Pushpendra Kumar

Copyright © 2016 S. Wang and G. Shao. This is an open access article distributed under the Creative Commons Attribution License, which permits unrestricted use, distribution, and reproduction in any medium, provided the original work is properly cited.

A number of carbide-derived carbon (CDC) samples were successfully synthesized by the electrolysis of SiC powder in molten CaCl_2 . The electrolysis was conducted at different temperatures (850, 900, and 950°C) for 48 h in argon at an applied constant voltage of 3.1 V. The structure of the resulting carbon is characterized by X-ray diffraction, Raman spectroscopy, and transmission electron microscope techniques. Cyclic voltammetry and galvanostatic charge/discharge measurements are applied to investigate electrochemical performances of the SiC-CDC material. It can be seen that the degree of order of the SiC-CDC increases monotonically along with elevation of reaction temperature, while the highest specific surface area $1137.74 \text{ m}^2/\text{g}$ together with a specific capacitance of 161.27 F/g at a current density 300 mA/g was achieved from sample synthesized at 900°C.

1. Introduction

Carbide-derived carbon (CDC) is a new class of nanoporous material produced by selective extraction of metal atoms from the carbide crystal lattice by halogens [1, 2], supercritical water [3], or thermal decomposition [4]. CDC is a promising candidate for applications as electric double-layer capacitors (EDLC) [5–7], ion batteries [8, 9], catalyst support [10], or storage of hydrogen [11].

Carbide-derived carbons (CDCs) made through chlorination of various metal carbides have been widely studied in recent years. However, chlorine gas is harmful to people and environment. So far, there have not been any reports on the preparation of SiC-CDC by fused salt electrolysis method. In this paper, SiC-CDC has been prepared by fused salt electrolysis method for the first time. In contrast to the conventional routes, especially the chlorination of metal carbides, this novel method is a much easier, safer, less expensive, and more environmentally friendly process. The as-prepared CDC in this work has high purity and specific capacitance and displays a superior electrocapacitive performance.

It is well known that the property of a material is greatly dependent upon its carbon onions structure. As described in

the literature, the CDC structure depends on the type of carbide precursor [12] and process parameters (e.g., temperature [13], chemical or physical activation [14], and catalysts [15]).

In this work, we have been successfully synthesized SiC-CDC powder by the electrolysis of SiC powder in molten CaCl_2 . The effects of different electrolysis temperatures on the degree of order and electrochemical performances of silicon carbide-derived carbon were also studied in detail. The different results from literature were achieved.

2. Experimental

2.1. Sample Preparation. Commercially available silicon carbide (SiC) powder (99.8%, 2.5~3.5 μm , Zhuzhou DeFeng Cemented Carbide Co. Ltd, China) was used as carbide precursor. The SiC powders were pressed into thin sheets of diameter of 8 mm and thickness of 1 mm with density of 29.86 g/cm^{-3} under a uniaxial pressure of 10 MPa and sintered in argon at 900°C for 12 h. The sintered SiC thin sheets were used as the anode for electrochemical production of SiC-CDC powders. A graphite rod ($d = 6 \text{ mm}$) served as the cathode. A DC power supply was employed for conducting electrolysis. The SiC thin sheets were led to the terminal

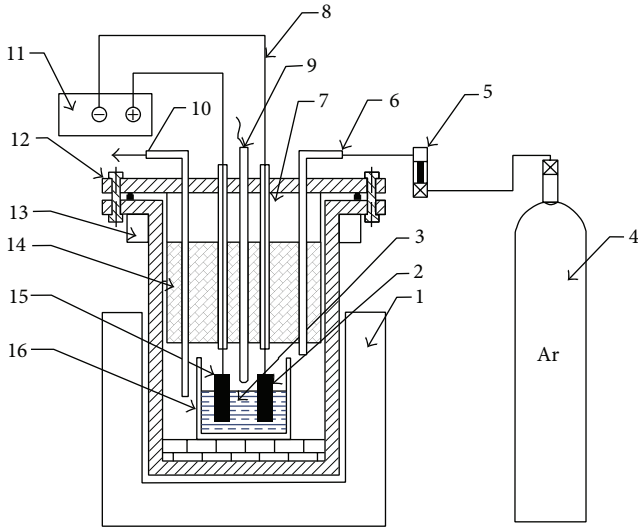


FIGURE 1: The schematic configuration of the equipment was as follows: (1) electric furnace, (2) cathode, (3) molten salt, (4) Ar gas, (5) flow meter, (6) Ar gas inlet, (7) cooling water, (8) electrode extension, (9) thermocouple, (10) Ar gas outlet, (11) regulated DC power source, (12) reactor, (13) cooling water, (14) thermal insulation layer, (15) anode, and (16) corundum crucible.

positive of the power supply. The negative terminal of the power supply was connected to the carbon cathode. Fused salt electrolysis was carried out at different temperatures for 48 h in argon at atmospheric pressure. The solid CaCl_2 melts at the temperature 778°C , and high temperature also results in high evaporation from the liquid CaCl_2 . As a result, the experimental temperatures 850°C , 900°C , and 950°C were selected. The constant voltage imposed to the cells was 3.1 V. After electrolysis, the furnace was cooled down to room temperature. The electrolytic products obtained from SiC anode were immersed in 1.5 M HCl for approximately 10 h. Then, the samples were rinsed with distilled water and dried in air at 120°C for 12 h.

The configuration of equipment is shown in Figure 1.

The electrolysis experiments were performed in a tubular stainless steel reactor, which was positioned vertically inside a programmable electrical furnace. A corundum crucible was filled with anhydrous calcium chloride and was heated in an argon atmosphere with a ramp rate $400^\circ\text{C}/\text{h}$ until the desired target temperature.

2.2. Characterization. The phases of the specimens were analyzed with the aid of three different techniques: (i) X-ray diffraction patterns between 10 (2θ) and 100 (2θ) degrees were collected by Rigaku D/MAX-2500 powder diffractometer with $\text{Cu-K}\alpha$ radiation ($\lambda = 0.154 \text{ nm}$) operated at 40 kV and 200 mA . (ii) Raman spectra from 100 cm^{-1} to 3200 cm^{-1} were recorded by using a Renishaw inVia Raman microscope instrument equipped with an Ar^+ laser ($\lambda = 514.5 \text{ nm}$) at $50\times$ magnification ($\sim 1 \mu\text{m}$ spot size) and 10% power. (iii) JEM 2010 transmission electron microscope (TEM) equipped with an imaging filter (Gatan GIF) was used at 200 kV . Specific surface area (SSA) and pore size distributions (PSD) were

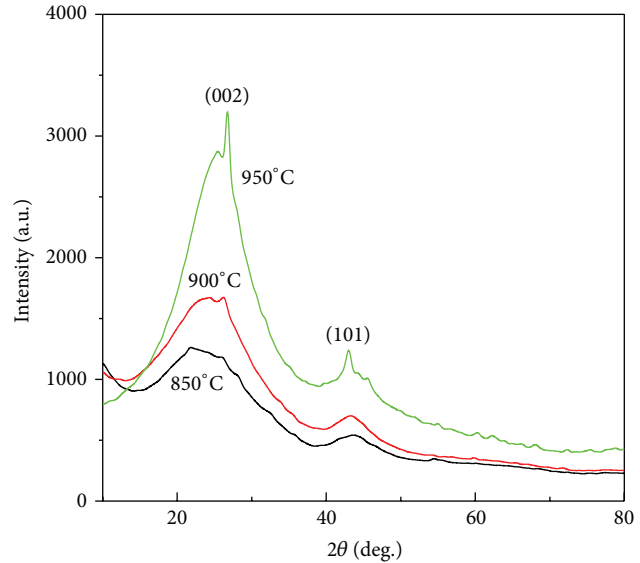


FIGURE 2: XRD patterns of the CDC electrolyzed at different temperatures of 850°C , 900°C , and 950°C .

tested using the specific surface analysis (ASAP 2010 V5.03H). Electrochemical investigations were carried out in a three-electrode cell using Platinum as counter electrode and Saturated Calomel Electrode (SCE) as reference electrode. The working electrodes were comprised of 94 wt\% CDC and 6 wt\% Polytetrafluoroethylene (PTFE) binder (10% suspension in water) and then pressed the slurry on a piece of foamed nickel grid whose area is $1 \times 1 \text{ cm}^2$. The total loading mass of active materials in each working electrode is 3 mg . The electrolytes containing 0.5 M Na_2SO_4 were used to study the capacitive behavior of prepared electrodes. Cyclic voltammetry (CV) studies were performed at a potential range of $-1.0 \sim -0.28 \text{ V}$ versus SCE at scan rates 5 mV/s . Galvanostatic charge-discharge tests were conducted at current densities of 300 , 500 , 1000 , and 1500 mA/g between -1.0 V and -0.28 V versus SCE using cycling equipment (NEWARE, China).

3. Results and Discussion

The XRD patterns of the products obtained at different electrolysis temperatures are shown in Figure 2.

No peak from other compounds appears within the detection limit of XRD. It is found that the CDC from the raw SiC powders is mainly amorphous carbon at electrolysis temperature of 850°C . The peaks corresponding to the graphite (002) and (101) planes at 2θ about 26.3° and 43.5° appear with increasing electrolysis temperatures. When the electrolysis was carried out at 950°C , the strongly sharp peak of the graphite (002) and (101) planes indicates an increase of the degree of order. The detected peaks become sharper and stronger with increasing electrolysis temperatures, suggesting that increasing electrolysis temperatures of the SiC powders can improve the degree of order in the CDC.

Raman spectroscopy is a suitable method to determine the degree of order of carbon materials. Figure 3 shows

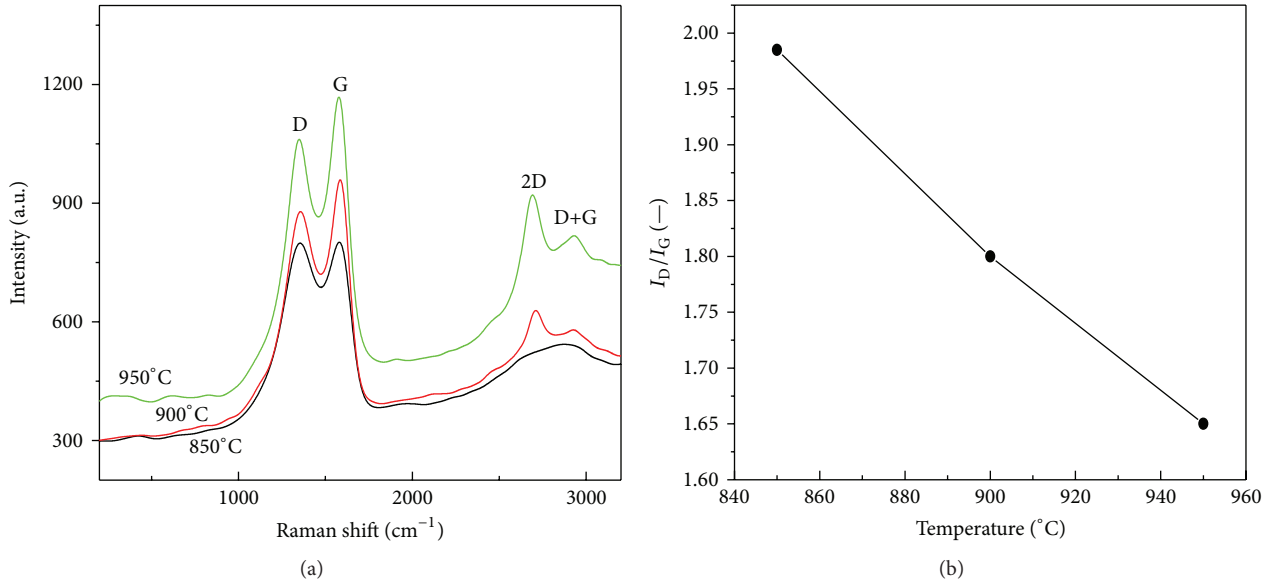


FIGURE 3: Raman spectra (a) and I_D/I_G (b) of the CDC electrolyzed at different temperatures.

the Raman spectra of the SiC-CDC obtained at different electrolysis temperatures.

The first-order Raman spectrum features two peaks: disorder-induced peak (D-band) at wavelength $\sim 1356\text{ cm}^{-1}$ and the graphite peak (G-band) at $\sim 1580\text{ cm}^{-1}$ are detected. And they become more and more sharp with increasing electrolysis temperature from 850°C to 950°C. The presence of D- and G-peaks and their intensity ratio (I_D/I_G) can be used to extract structural information of the carbon materials. The width and intensity of these two peaks suggest the disordered nature of carbon produced from SiC-CDC. The fitted area ratio of D-band to G-band (I_D/I_G) is 1.985, 1.8, and 1.65, respectively [16]. In addition, the spectrum also shows two marked second-order peaks of the D-band (2D) at $\sim 2695\text{ cm}^{-1}$ as well as (D+G) band at $\sim 2930\text{ cm}^{-1}$ for the SiC-CDC from electrolysis temperatures 900°C and 950°C. The increase of second-order peaks is related to the ordering of the graphitic structure. Raman analysis of the samples indicates that the degree of order of SiC-CDC increases along with elevation of reaction temperature and the degree of order of this SiC-CDC is much higher than those reported CDCs in literatures [17].

The degree of order of CDC was further studied by TEM technology. Figure 4 shows TEM images of the CDCs from SiC powders electrolyzed at different temperatures. The images directly reflect the effect of temperature on the microstructure of CDCs. It can be seen that, in Figures 4(a) and 4(b), the CDC from the raw SiC powder electrolysis at 850°C is mainly amorphous carbon, and no graphitic ribbons were found. At 900°C, along with the presence of amorphous carbon with thin sheet, the formation of some graphitic ribbons (Figures 4(c) and 4(d)) was seen obviously. As the electrolysis temperature further increases, at 950°C (Figures 4(e) and 4(f)), CDC contained less amorphous carbon and a large amount of highly ordered curved sheets of graphite with

an interplanar distance of 0.339 nm, which is corresponding to the interplanar spacing of (002). The images directly reflect that SiC-CDC is a mixture of amorphous carbon and ordered graphite phase with a high degree of graphitization at higher electrolysis temperature. The TEM images are in full agreement with the XRD and Raman spectroscopy patterns.

CV tests were conducted to characterize the electrochemical performances of SiC-CDC. In Figure 5(a), no faradic reactions were found within the voltage window of interest for all samples. They exhibit almost rectangular shape characteristic. And the rectangular area of the SiC-CDC electrolysis at 900°C is the largest among the three samples. The charge-discharge plots of the SiC-CDC were shown in Figure 5(b); as can be seen, all the charge/discharge profiles are close to an isosceles triangle, which indicates fine capacitive and revisable behaviors of the SiC-CDC. The calculated specific capacitance of synthesized samples varied with different temperatures; however, the results did not follow the trend of I_D/I_G (Figure 3(b)). The highest specific capacitance of 161.27 F/g was achieved in the sample obtained at 900°C, which is significantly higher than 100 F/g for conventional activated carbons and 138.3 F/g, 115 F/g, and 120 F/g, the maximum specific capacitance of the samples synthesized by chlorination of carbides in literatures [18–20], and goes down to 143.04 F/g in the sample obtained at 950°C. The calculated energy density at the temperature of 900°C is 22.4 Wh/kg.

It has been reported that a lot of factors of porous carbon can affect double-layer capacitance, for example, surface areas, microstructures, and pore sizes as well as pore shapes [19]. The porous structure of SiC-CDC prepared has been characterized using the low-temperature nitrogen sorption method within the relative pressure range from 10^{-7} to 0.95. The specific surface area, S_{BET} , is calculated according to Brunauer-Emmett-Teller (BET) theory, although it might not be best suited for analyzing CDC materials due to large errors

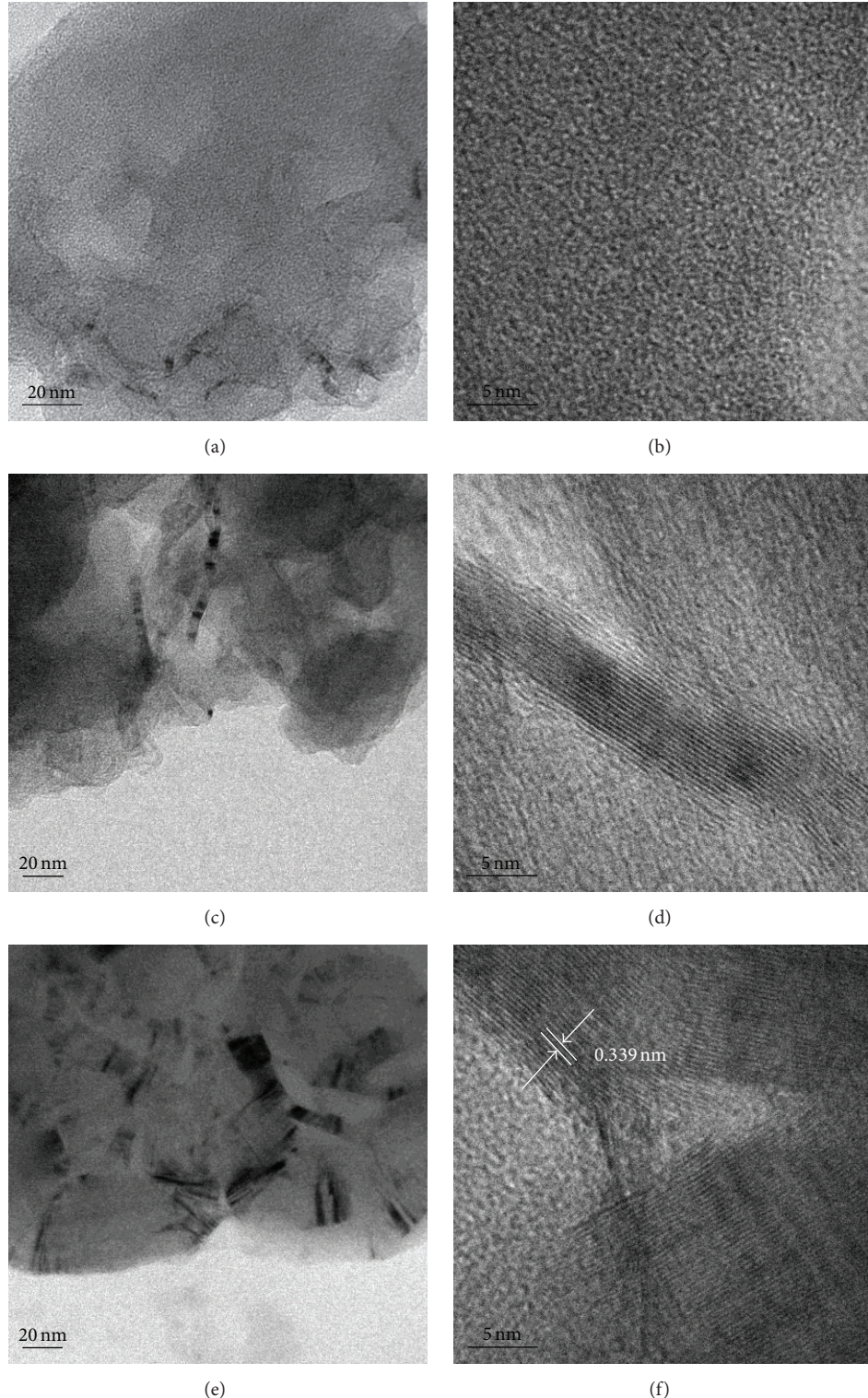


FIGURE 4: TEM images of the CDC: (a-b) electrolyzed at 850°C, (c-d) at 900°C, and (e-f) at 950°C.

arising from wrong parameters assumed during analysis of the data [21]. The total BET surface area for the SiC-CDC from different electrolysis temperatures 850°C, 900°C, and 950°C is 763.84 m²/g, 1137.74 m²/g, and 988.55 m²/g, respectively.

The pore size distributions (Figure 6) of the samples have been calculated applying Horvath-Kawazoe theory. It indicates the coexistence of micropores (pore < 2 nm) and mesopores (pores in between 2 and 50 nm) in these SiC-CDCs. In addition, we also notice that the SiC-CDC synthesized

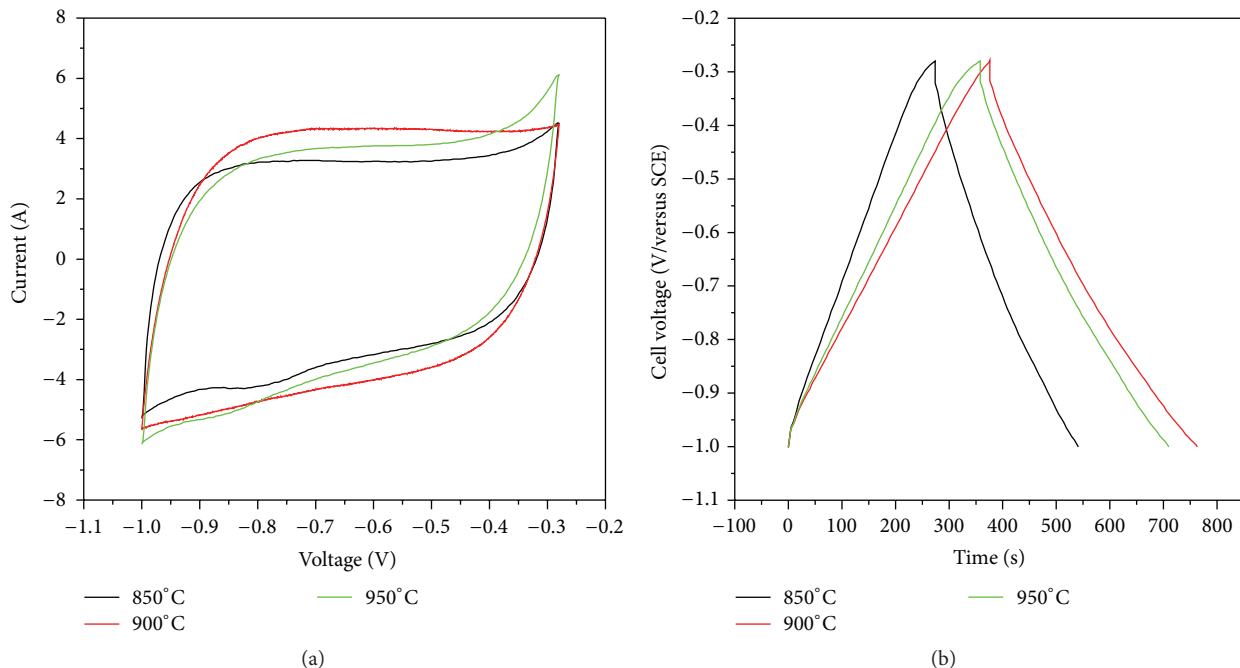


FIGURE 5: (a) Cyclic voltammogram of SiC-CDC electrolyzed at different temperatures with sweep rate of 5 mV/s; (b) charge-discharge curves measured at 300 mA/g.

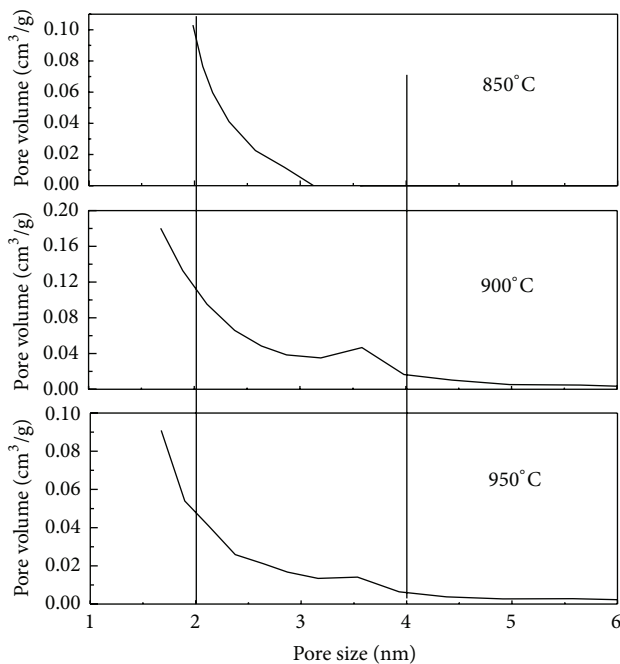


FIGURE 6: Pore size distributions of SiC-CDC electrolyzed at different temperatures.

at electrolysis temperature 900°C has the highest proportion of pore volume and micropores in three samples. The high proportion micropores in the CDC help to enhance double-layer capacitance [17]. As a result, the sample synthesized at electrolysis temperature 900°C exhibits the largest specific surface area and the highest specific capacitance.

4. Conclusions

The SiC-CDC has been successfully synthesized by electrolysis of SiC powder in molten CaCl₂. This method to produce SiC-CDC is a much easier, safer, less expensive, and more environmentally friendly process. The as-prepared CDC has much higher purity and specific capacitance and displays a superior electrocapacitive performance.

We also studied the effects of different electrolysis temperatures on the degree of order and electrochemical performance of SiC-CDC. It is demonstrated that the degree of order of the SiC-CDC increases monotonically along with elevation of reaction temperature, and the highest degree of order occurs at the electrolysis temperature 950°C. The highest specific capacitance of 161.27 F/g at a current density 300 mA/g was achieved from the sample synthesized at 900°C, which is significantly higher than the chlorination of carbides synthesized samples. This improved design provides a more economic way to produce CDC with good specific supercapacitance.

Competing Interests

The authors declare that they have no competing interests.

References

- [1] I. Tallo, T. Thomberg, K. Kontturi, A. Jänes, and E. Lust, "Nanosstructured carbide-derived carbon synthesized by chlorination of tungsten carbide," *Carbon*, vol. 49, no. 13, pp. 4427–4433, 2011.
- [2] P. González-García, E. Urones-Garrote, E. del Corro, D. Ávila-Brande, and L. C. Otero-Díaz, "The production of carbon

- particles of different shapes produced by the chlorination of $\text{Cr}(\text{C}_5\text{H}_5)_2$,” *Carbon*, vol. 52, pp. 90–99, 2013.
- [3] Y. G. Gogotsi, P. Kofstad, M. Yoshimura, and K. G. Nickel, “Formation of sp₃-bonded carbon upon hydrothermal treatment of SiC,” *Diamond and Related Materials*, vol. 5, no. 2, pp. 151–162, 1996.
- [4] S. Iijima, “Graphitization of silicon carbide due to electron beam irradiation,” *Journal of Solid State Chemistry*, vol. 42, no. 1, pp. 101–105, 1982.
- [5] P. Simon and Y. Gogotsi, “Materials for electrochemical capacitors,” *Nature Materials*, vol. 7, no. 11, pp. 845–854, 2008.
- [6] M. Inagaki, H. Konno, and O. Tanaike, “Carbon materials for electrochemical capacitors,” *Journal of Power Sources*, vol. 195, no. 24, pp. 7880–7903, 2010.
- [7] W. Li, D. Chen, Z. Li et al., “Nitrogen enriched mesoporous carbon spheres obtained by a facile method and its application for electrochemical capacitor,” *Electrochemistry Communications*, vol. 9, no. 4, pp. 569–573, 2007.
- [8] C. Li, X. Yin, L. Chen, Q. Li, and T. Wang, “Porous carbon nanofibers derived from conducting polymer: synthesis and application in lithium-ion batteries with high-rate capability,” *The Journal of Physical Chemistry C*, vol. 113, no. 30, pp. 13438–13442, 2009.
- [9] L. Ji and X. Zhang, “Fabrication of porous carbon/Si composite nanofibers as high-capacity battery electrodes,” *Electrochemistry Communications*, vol. 11, no. 6, pp. 1146–1149, 2009.
- [10] D. A. Ersoy, M. J. McNallan, and Y. Gogotsi, “Platinum reactions with carbon coatings produced by high temperature chlorination of silicon carbide,” *Journal of the Electrochemical Society*, vol. 148, no. 12, pp. C774–C779, 2001.
- [11] R. Dash, J. Chmiola, G. Yushin et al., “Titanium carbide derived nanoporous carbon for energy-related applications,” *Carbon*, vol. 44, no. 12, pp. 2489–2497, 2006.
- [12] M. Kormann, H. Gerhard, and N. Popovska, “Comparative study of carbide-derived carbons obtained from biomorphic TiC and SiC structures,” *Carbon*, vol. 47, no. 1, pp. 242–250, 2009.
- [13] C. Portet, D. Kazachkin, S. Osswald, Y. Gogotsi, and E. Borguet, “Impact of synthesis conditions on surface chemistry and structure of carbide-derived carbons,” *Thermochimica Acta*, vol. 497, no. 1-2, pp. 137–142, 2010.
- [14] M. Kormann and N. Popovska, “Processing of carbide-derived carbons with enhanced porosity by activation with carbon dioxide,” *Microporous and Mesoporous Materials*, vol. 130, no. 1–3, pp. 167–173, 2010.
- [15] M. Kormann, H. Gerhard, C. Zollfrank, H. Scheel, and N. Popovska, “Effect of transition metal catalysts on the microstructure of carbide-derived carbon,” *Carbon*, vol. 47, no. 10, pp. 2344–2351, 2009.
- [16] J. Ribeiro-Soares, L. G. Cançado, N. P. S. Falcão, E. H. Martins Ferreira, C. A. Achete, and A. Jorio, “The use of Raman spectroscopy to characterize the carbon materials found in Amazonian anthrosols,” *Journal of Raman Spectroscopy*, vol. 44, no. 2, pp. 283–289, 2013.
- [17] A. Jänes, T. Thomberg, and E. Lust, “Synthesis and characterisation of nanoporous carbide-derived carbon by chlorination of vanadium carbide,” *Carbon*, vol. 45, no. 14, pp. 2717–2722, 2007.
- [18] Y. Zhao, W. Wang, D.-B. Xiong et al., “Titanium carbide derived nanoporous carbon for supercapacitor applications,” *International Journal of Hydrogen Energy*, vol. 37, no. 24, pp. 19395–19400, 2012.
- [19] E. Tee, I. Tallo, H. Kurig, T. Thomberg, A. Jänes, and E. Lust, “Huge enhancement of energy storage capacity and power density of supercapacitors based on the carbon dioxide activated microporous SiC-CDC,” *Electrochimica Acta*, vol. 161, pp. 364–370, 2015.
- [20] T. Ariyanto, A. M. Laziz, J. Gläsel, G.-R. Zhang, J. Garbes, and B. J. M. Etzold, “Producing high quality carbide-derived carbon from low quality byproducts stemming from SiC production,” *Chemical Engineering Journal*, vol. 283, pp. 676–681, 2016.
- [21] F. Stoeckli and T. A. Centeno, “On the determination of surface areas in activated carbons,” *Carbon*, vol. 43, no. 6, pp. 1184–1190, 2005.



Journal of
Nanotechnology



International Journal of
Corrosion



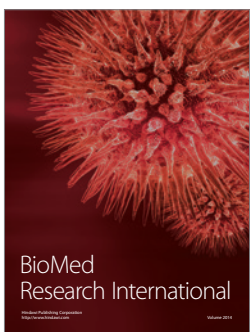
International Journal of
Polymer Science



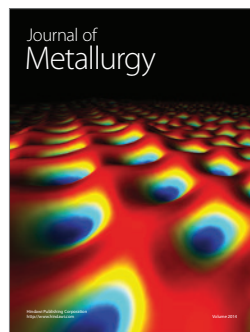
Smart Materials
Research



Journal of
Composites



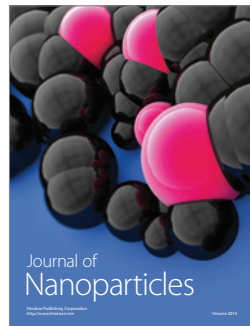
BioMed
Research International



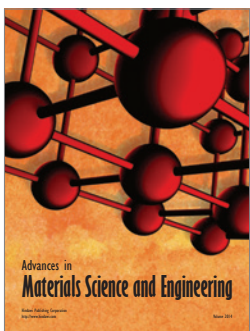
Journal of
Metallurgy



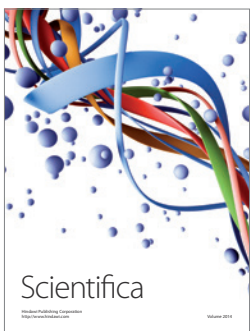
Journal of
Materials



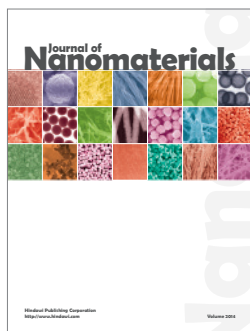
Journal of
Nanoparticles



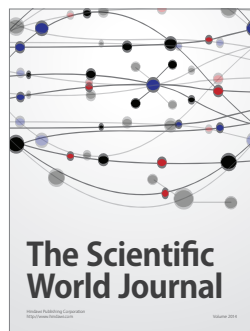
Advances in
Materials Science and Engineering



Scientifica



Journal of
Nanomaterials



The Scientific
World Journal



International Journal of
Biomaterials



Journal of
Nanoscience



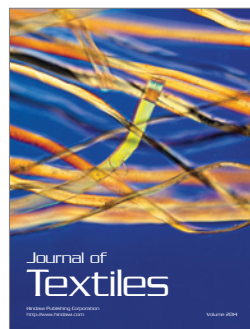
Journal of
Coatings



Journal of
Crystallography



Journal of
Ceramics



Journal of
Textiles